ISSN: 0256-307X

中国物理快报

Chinese Physics Letters

Volume 29 Number 9 September 2012

A Series Journal of the Chinese Physical Society
Distributed by IOP Publishing

Online: http://iopscience.iop.org/cpl
http://cpl.iphy.ac.cn

CHINESE PHYSICAL SOCIETY
IOP Publishing

CHIN. PHYS. LETT. Vol. 29, No. 9 (2012) 097701

Exchange Bias in Polycrystalline $BiFe_{1-x}Mn_xO_3/Ni_{81}Fe_{19}$ Bilayers *

YUAN Xue-Yong(袁学勇)[1], XUE Xiao-Bo(薛晓波)[2], SI Li-Fang(司丽芳)[1],
DU Jun(杜军)[2], XU Qing-Yu(徐庆宇)[1,3]**

[1]*Department of Physics, Southeast University, Nanjing 211189*
[2]*National Laboratory of Solid State Microstructures and Department of Physics, Nanjing University, Nanjing 210093*
[3]*Key Laboratory of MEMS of the Ministry of Education, Southeast University, Nanjing 210096*

(Received 4 July 2012)

Polycrystalline $BiFe_{1-x}Mn_xO_3$ films with x up to 0.50 are prepared on $LaNiO_3$ buffered surface oxidized Si substrates. The doped Mn is confirmed to be partially in a +4 valence state. A clear exchange bias effect is observed with a 3.6 nm $Ni_{81}Fe_{19}$ layer deposited on the top $BiFe_{1-x}Mn_xO_3$ layer, which decreases drastically with increasing Mn doping concentration and finally to zero when x is above 0.20. These results clearly demonstrate that the exchange bias field comes from the net spins due to the canted antiferromagnetic spin structure in polycrystalline $BiFe_{1-x}Mn_xO_3$ films, which transforms to a collinear antiferromagnetic spin structure when the Mn doping concentration is larger than 0.20.

PACS: 77.55.Nv, 75.30.Et, 75.50.Ee DOI: 10.1088/0256-307X/29/9/097701

Multiferroic materials which present simultaneously ferroelectric and magnetic orderings have attracted extensive interest due to their abundant physics and potential applications in novel devices.[1] However, room-temperature multiferroic materials are very rare. $BiFeO_3$ is an antiferromagnetic-ferroelectric compound at room temperature (Neel temperature T_N~643 K and Curie temperature T_C~1103 K).[2] The coupling between the antiferromagnetic and ferroelectric orderings has been confirmed experimentally by the observation of coupled ferroelectric and antiferromagnetic domains.[3] At room temperature, it has a rhombohedral *R3c* perovskite structure with a large electric polarization (60 $\mu C/cm^2$) pointing along the elongated [111] direction.[4]

In bulk $BiFeO_3$, the Fe^{3+} spins order in a G-type antiferromagnetic structure with a superimposed long-wavelength (~62 nm) cycloidal modulation.[5] However, $BiFeO_3$ thin films might show rather different properties from those of bulk samples. Many studies have been devoted to epitaxially grown single crystalline $BiFeO_3$ films.[6] The cycloidal spin structure was destroyed due to the epitaxial strains in single crystalline $BiFeO_3$ films.[7] Due to the antiferromagnetic nature of $BiFeO_3$, the most plausible application in spintronics is suggested to be an antiferromagnetic pinning layer.[8] The exchange bias has been mostly reported in epitaxial single crystalline $BiFeO_3$ with various ferromagnetic layers, such as NiFe, CoFeB, CoFe, $La_{0.7}Sr_{0.3}MnO_3$, and Fe_3O_4.[9–18] Due to the complicated spin structure and magnetoelectric coupling in $BiFeO_3$, the mechanism of the exchange bias is still under debate. The surface roughness,[11] 109° ferroelectric domain walls,[12] antiferromagnetic domain size,[13] canted magnetic moment of $BiFeO_3$ near the interface due to the interface exchange coupling,[15,16] spin canting of $BiFeO_3$,[17] etc. have been proposed to explain the exchange bias. Therefore, further studies are still needed to clarify the mechanism.

Furthermore, studies on polycrystalline $BiFeO_3$ are still rare.[19,20] In this Letter, the exchange bias effect in polycrystalline $BiFe_{1-x}Mn_xO_3/Ni_{81}Fe_{19}$ (NiFe) bilayers is systematically investigated. The drastic decrease of exchange bias field with increasing Mn concentration indicates that the exchange bias field comes from the spin canting due to the canted antiferromagnetic spin structure in polycrystalline $BiFe_{1-x}Mn_xO_3$ films, which transforms to a collinear antiferromagnetic spin structure when x is above 0.20.

The $BiFe_{1-x}Mn_xO_3$ (x = 0, 0.05, 0.1, 0.2, 0.3, 0.5) targets were prepared by the tartaric acid modified sol-gel method.[21] The bilayer of $BiFe_{1-x}Mn_xO_3$/NiFe (~80 nm and 3.6 nm in thickness, respectively) magnetic heterostructures were deposited on surface oxidized Si (100) substrates by pulsed laser deposition (PLD) for the oxide layers and magnetron sputtering for the metallic layers, as described previously.[20] Before the growth of $BiFe_{1-x}Mn_xO_3$, a $LaNiO_3$ buffer layer (~30 nm thick) was first deposited by PLD. Finally, Ta as the capping layer for preventing the NiFe layer from oxidization

*Supported by the National Basic Research Program of China under Grant Nos 2010CB923404 and 2010CB923401, the National Natural Science Foundation of China (51172044, 11074112, 11174131), the National Science Foundation of Jiangsu Province (BK2011617, BK2010421), the New Century Excellent Talent Project of the Ministry of Education of China under Grant No NCET-09-0296, the Scientific Research Foundation for the Returned Overseas Chinese Scholars, State Education Ministry, and Southeast University (the Excellent Young Teachers Program and Seujq201106).

**Corresponding author. Email: xuqingyu@seu.edu.cn

was deposited. The thickness of the $BiFe_{1-x}Mn_xO_3$ films was controlled by the number of laser pulses and calibrated by a transmission electron microscope. The crystal structure of the films was examined by x-ray diffraction (XRD) with Cu Kα radiation. X-ray photoelectron spectroscopy (XPS, ThermoFisher SCIENTIFIC) with an Al Kα x-ray source ($h\nu$=1486.6 eV), and calibrated by the C 1s line (284.8 eV) binding energy.[22] Raman measurements were carried out on a Horiba Jobin Yvon LabRAM HR 800 micro-Raman spectrometer with 785 nm excitation under air ambient conditions at room temperature. The magnetic hysteresis (M–H) loops were measured by a vibrating sample magnetometer (VSM, Microsense EV7) at room temperature with an applied field parallel to the film plane.

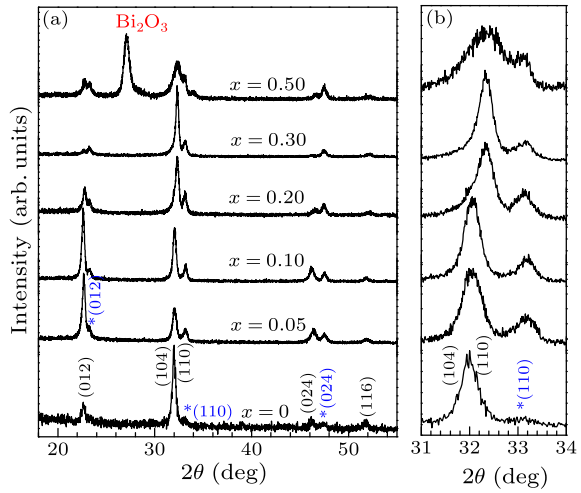

Fig. 1. XRD patterns of (a) $LaNiO_3/BiFe_{1-x}Mn_xO_3$ (x = 0, 0.05, 0.10, 0.20, 0.30, 0.50) bilayers. The asterisks denote the diffraction peaks from $LaNiO_3$, the impurity peak has been indexed to Bi_2O_3, and the rest are from $BiFeO_3$. (b) The magnified view in the vicinity of $2\theta = 32°$.

Figure 1 shows the XRD patterns of $BiFe_{1-x}Mn_xO_3$ films on SiO_2/Si (100) substrates with $LaNiO_3$ as the buffer layer. The pseudocubic lattice constant is 3.84 Å for $LaNiO_3$[23] and 3.96 Å for $BiFeO_3$.[24] Thus the polycrystalline $BiFeO_3$ might be epitaxially grown on the $LaNiO_3$ grains, as indicated in our previous report.[20] Besides the diffraction peaks corresponding to $LaNiO_3$, all the other peaks can be indexed to the $BiFeO_3$ of a pure $R3c$ structure with x increasing from 0 to 0.30. With further increase of x up to 0.50, a strong impurity peak of Bi_2O_3 can be clearly observed, though the remaining peaks can still be indexed to the $R3c$ structure. These results are consistent with the previous report.[25] Figure 1(b) shows the magnified patterns around $2\theta = 32°$. The (104) and (110) peaks both shift to higher angles with increasing Mn doping concentration, which is consistent with the previous report on bulk $BiFe_{1-x}Mn_xO_3$ ceramics.[26] The Mn 2p XPS spectrum of the $BiFe_{0.95}Mn_{0.05}O_3$ film was taken to study the valence state of the doped Mn ions, as shown in Fig. 2(a). The binding energy of Mn $2p_{3/2}$ in MnO, Mn_2O_3 and Mn_3O_4 are between 641 and 641.5 eV, while that of MnO_2 is around 642 eV.[27] The binding energy of Mn $2p_{3/2}$ at 641.7 eV indicates that the doped Mn ions are partially in a +4 valence state. The radius of Mn^{+4} (0.67 Å) is smaller than that of Fe^{+3} (0.69 Å),[28] leading to decrease of the lattice constant. This result indicates that the lattice parameter is changed by Mn substitution and a gradual phase transition from the rhombohedral distortion to orthorhombic or tetragonal structure with the increase of Mn doping content, as reported by Singh *et al.*[29] Furthermore, the substituted Mn ions in a +4 valence state will suppress the O vacancies due to charge compensation, leading to the effective suppression of the leakage current and improved ferroelectricity.[18] Figure 2(b) shows the Fe 2p XPS spectrum of Fe. The binding energy of Fe $2p_{3/2}$ is at 709.9 eV, suggesting the existence of Fe^{2+}.[27] However, the decomposition of the Fe $2p_{3/2}$ spectrum into a superposition of symmetric components is questionable, thus it is complicated to obtain the exact concentration of Fe^{2+}.[30] The clear observation of the satellite peaks and the similar curve shape to that of Fe_2O_3 indicate that Fe ions are mainly in the +3 valence state.[30]

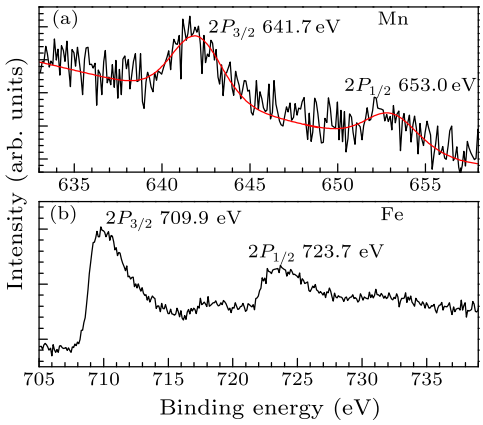

Fig. 2. The Mn 2p (a) and Fe 2p (b) XPS spectra for the $BiFe_{0.95}Mn_{0.05}O_3$ film.

Figure 3 shows the Raman spectra of polycrystalline $BiFe_{1-x}Mn_xO_3$ films. Except for the strong peak at 520 cm^{-1} corresponding to the Si substrate,[31] the clearly resolved Raman modes can all be indexed to the modes of $BiFeO_3$ with the $R3c$ structure.[32] The A_1-1, A_1-2 and A_1-3 modes are associated with the Bi-O vibrations. Their peak intensities decrease with increasing Mn concentration, and nearly disappear with x above 0.20. This indicates that a phase transition may occur when x is above 0.20,[33] which is consistent with the XRD result. Compared with

the pure $BiFeO_3$ film, two strong and wide bands can be clearly observed, i.e., one at 620 cm^{-1} and the other in the range from 450 cm^{-1} to 550 cm^{-1} in the $BiFe_{1-x}Mn_xO_3$ films. These two distinct bands have been attributed to the distortion of $[(Mn, Fe)^{3+}O_6]$ octahedral.[34]

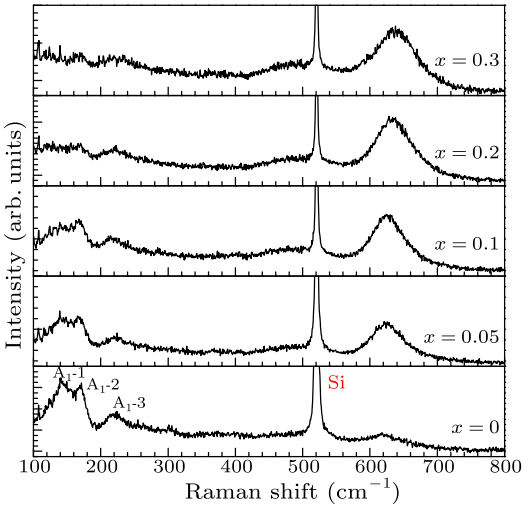

Fig. 3. Raman spectra of $LaNiO_3/BiFe_{1-x}Mn_xO_3$ (x = 0, 0.05, 0.10, 0.20, 0.30) bilayers.

In order to obtain a sizeable exchange bias, 3.6 nm NiFe thin films were deposited on the $BiFe_{1-x}Mn_xO_3$ films. The corresponding M–H loops are shown in Fig. 4. It can be clearly seen that the central position of M–H loops exhibit a shift (exchange bias field, H_E) towards a negative field with the increasing Mn doping concentration up to 0.20. When the substitution of Mn increases up to 0.30 or even larger, the exchange bias field vanishes. The inset of Fig. 4 shows the dependences of the exchange bias field and coercivity on Mn doping concentration. It shows that the exchange bias field decreases drastically even with only 5% Mn doping. The coercivity also shows a decrease with increasing Mn doping concentration. A similar phenomenon has been reported previously by Allibe *et al.* on $BiFeO_3$/CoFeB bilayers, i.e., the exchange bias field decreases from 51 Oe to 25 Oe and the coercivity decreases from 42 Oe to 17 Oe with only 5% Mn doping.[18]

Generally, the exchange bias was attributed to the exchange interaction between the pinned uncompensated spins in the antiferromagnet and the magnetic moments in the ferromagnet, whereas the increase in the coercivity of the ferromagnet has been related to some coupling between unpinned uncompensated spins and ferromagnetic moments.[18] The decrease of the exchange bias field and coercivity might be attributed to the decrease of the uncompensated spins at the ferromagnet/antiferromagent interface. $BiFeO_3$ basically has a G-type antiferromagnetic spin arrangement with canted neighboring spins. Lebeugle *et al.*[17] have suggested that the uncompensated spins at the interface is due to the local spin canting in $BiFeO_3$. It has been further demonstrated by Heron *et al.* in the electrical field manipulation of the magnetization of a CoFe layer on $BiFeO_3$ film that the spin of the ferromagnetic layer lies parallel to the net spin of the canted spins.[35] The neutron diffraction study shows that Mn doping results in a transformation from a long-range spiral spin modulation of $BiFeO_3$ to a collinear antiferromagnetic spin structure with increasing Mn concentration beyond 0.20,[36] which would lead to the decrease of net spins at the interface. Based on the above discussions, we can conclude that the Mn doping will suppress the local spin canting. Therefore, the net spin at the ferromagnet/$BiFeO_3$ interface will decrease with increasing Mn doping concentration, leading to a decrease of the exchange bias field and coercivity.

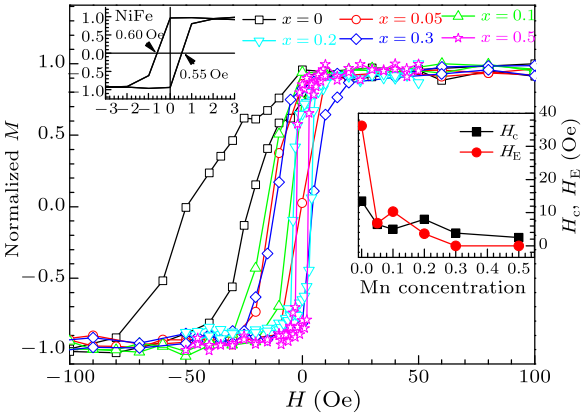

Fig. 4. M–H curves of $BiFe_{1-x}Mn_xO_3$/NiFe (x = 0, 0.05, 0.10, 0.20, 0.30, 0.50) bilayers at room temperature. The left top inset shows the M–H curve of a single NiFe layer (3.6 nm thick), confirming that the residual field of the magnet is nearly zero (<0.1 Oe). The right bottom inset shows the dependences of the exchange bias field and coercivity on Mn doping concentration.

In conclusion, we have systematically studied the exchange bias in polycrystalline $BiFe_{1-x}Mn_xO_3$/NiFe bilayers. The XPS results have confirmed that the doped Mn ions are partially in a +4 valence state. The exchange bias field decreases drastically with increasing Mn doping concentration and finally to zero when x is above 0.20. These results clearly demonstrate that the interface exchange bias field comes from the interfacial net spins due to the canted antiferromagnetic spin structure in polycrystalline $BiFe_{1-x}Mn_xO_3$ films. The drastic decrease of exchange bias is due to the transformation to a collinear antiferromagnetic spin structure with increasing Mn doping concentration.

References

[1] Spaldin N A and Fiebig M 2005 *Science* **309** 391

[2] Catalan G and Scott J F 2009 *Adv. Mater.* **21** 2463
[3] Zhao T, Scholl A, Zavaliche F, Lee K, Barry M, Doran A, Cruz M P, Chu Y H, Ederer C, Spaldin N A, Das R R, Kim D M, Baek S H, Eom C B and Ramesh R 2006 *Nat. Mater.* **5** 823
[4] Lebeugle D, Colson D, Forget A, Viret M, Bonville P, Marucco J F and Fusil S 2007 *Phys. Rev.* B **76** 024116
[5] Sosnowska I, Peterlin-Neumaier T and Steichele E 1982 *J. Phys.* C **15** 4835
[6] Béa H, Bibes M, Fusil S, Bouzehouane K, Jacquet E, Rode K, Bencok P and Barthélémy A 2006 *Phys. Rev.* B **74** 020101(R)
[7] Béa H, Bibes M, Petit S, Kreisel J and Barthélémy A 2007 *Philos. Mag. Lett.* **87** 165
[8] Bibes M and Barthélémy 2008 *Nat. Mater.* **7** 425
[9] Naganuma H, Oogane M and Ando Y 2011 *J. Appl. Phys.* **109** 07D736
[10] Béa H, Bibes M, Cherifi S, Nolting F, Warot-Fonrose B, Fusil S, Herranz G, Deranlot C, Jacquet E, Bouzehouzne K and Barthélémy A 2006 *Appl. Phys. Lett.* **89** 242114
[11] Dho J and Blamire M G 2009 *J. Appl. Phys.* **106** 073914
[12] Martin L W, Chu Y H, Holcomb M B, Huijben M, Yu P, Han S, Lee D, Wang S X and Ramesh R 2008 *Nano Lett.* **8** 2050
[13] Béa H, Bibes M, Ott F, Dupé B, Zhu X H, Petit S, Fusil S, Deranlot C, Bouzehouane K and Barthélémy A 2008 *Phys. Rev. Lett.* **100** 017204
[14] Wu S M, Cybart S A, Yu P, Rossell M D, Zhang J X, Ramesh R and Dynes R C 2010 *Nat. Mater.* **9** 756
[15] Yu P, Lee J S, Okamoto S, Rossell M D Huijben M, Yang C H, He Q, Zhang J X, Yang S Y, Lee M J, Ramasse Q M, Erni R, Chu Y H, Arena D A, Kao C C, Martin L W and Ramesh R 2010 *Phys. Rev. Lett.* **105** 027201
[16] Qu T L, Zhao Y G, Yu P, Zhao H C, Zhang S and Yang L F 2012 *Appl. Phys. Lett.* **100** 242410
[17] Lebeugle D, Mougin A, Viret M, Colson D and Ranno L 2009 *Phys. Rev. Lett.* **103** 257601
[18] Allibe J, Infante I C, Fusil S, Bouzehouane K, Jacquet E, Deranlot C, Bibes M and Barthélémy A 2009 *Appl. Phys. Lett.* **95** 182503
[19] Hauguel T, Pogossian S P, Dekadjevi D T, Spenato D, Jay J, Indenbom M V and Youssef J B 2011 *J. Appl. Phys.* **110** 073906
[20] Yuan X, Xue X, Zhang X, Wen Z, Yang M, Du J, Wu D and Xu Q 2012 *Solid State Commun.* **152** 241
[21] Xu Q, Zheng X, Wen Z, Yang Y, Wu D and Xu M 2011 *Solid State Commun.* **151** 624
[22] Wei L, Li Z and Zhang W F 2009 *Appl. Surf. Sci.* **255** 4992
[23] Miyazaki H, Goto T, Miwa Y, Ohno T, Suzuki H, Ota T and Takahashi M 2004 *J. Eur. Ceram. Soc.* **24** 1005
[24] Zavaliche F, Yang S Y, Zhao T, Chu Y H, Cruz M P, Eom C B and Ramesh R 2006 *Phase Trans.* **79** 991
[25] Singh S K, Ishiwara H and Maruyama K 2006 *Appl. Phys. Lett.* **88** 262908
[26] Ianculescu A, Gheorghiu F P, Postolache P, Oprea O and Mitoseriu L 2010 *J. Alloys Compd.* **504** 420
[27] Wagner C D, Riggs W M, Davis L E, Moulder J F and Muilenberg G E 1979 *Handbook X-Ray Photoelectron Spectroscopy* (Perkin-Elmer Corporation) pp 74–77
[28] Shannon R D 1976 *Acta. Cryst.* A **32** 751
[29] Singh S K, Ishiwara H, Sato K and Maruyama K 2007 *J. Appl. Phys.* **102** 094109
[30] Kozakov A T, Kochur A G, Googlev K A, Nikolsky A V, Raevski I P, Smotrakov V G and Yeremkin V V 2011 *J. Electron Spectrosc. Relat. Phenom.* **184** 16
[31] Wang Y, Lin Y and Nan C 2008 *J. Appl. Phys.* **104** 123912
[32] Hermet P, Goffinet M, Kreisel J and Ghosez Ph 2007 *Phys. Rev.* B **75** 220102(R)
[33] Wen Z, You L, Shen X, Li X, Wu D, Wang J and Li A 2011 *Mater. Sci. Eng.* B **176** 990
[34] Huang J, Shen Y, Li M and Nan C 2011 *J. Appl. Phys.* **110** 094106
[35] Heron J T, Trassin M, Ashraf K, Gajek M, He Q, Yang S Y, Nikonov D E, Chu Y H, Salahuddin S and Ramesh R 2011 *Phys. Rev. Lett.* **107** 217202
[36] Sosnowska I, Schäfer W, Kocklmann W, Andersen K H and Troyanchuk I O 2002 *Appl. Phys.* A **74** S1040

Chinese Physics Letters

Volume 29 Number 9 September 2012

PHYSICS OF GASES, PLASMAS, AND ELECTRIC DISCHARGES

CONDENSED MATTER: STRUCTURE, MECHANICAL AND THERMAL PROPERTIES

CONDENSED MATTER: ELECTRONIC STRUCTURE, ELECTRICAL, MAGNETIC, AND OPTICAL PROPERTIES

CROSS-DISCIPLINARY PHYSICS AND RELATED AREAS OF SCIENCE AND TECHNOLOGY

GEOPHYSICS, ASTRONOMY, AND ASTROPHYSICS